

## Supporting Information

### The temperature-controlled optimization of g-C<sub>3</sub>N<sub>4</sub> structure significantly enhances the efficiency of photothermal catalytic NO removal †

Kai Qi,<sup>abc</sup> Guoqiang Tan,<sup>\*b</sup> Zihan Lu,<sup>cd</sup> Xiangyu Gao,<sup>c</sup> Zhuoyuan Zhang,<sup>cd</sup> Dan Liu,<sup>cd</sup> Rui Lv,<sup>cd</sup> Da Jing,<sup>c</sup>  
Peng Luo,<sup>c</sup> and Guohui Dong<sup>\*a</sup>

---

<sup>a</sup> Shaanxi Key Laboratory of Green Preparation and Functionalization for Inorganic Materials, School of Materials Science and Engineering, Shaanxi University of Science & Technology, Xi'an 710021, China. E-mail: [dongguohui@sust.edu.cn](mailto:dongguohui@sust.edu.cn) ; [tan3114@163.com](mailto:tan3114@163.com)

<sup>b</sup> School of Environmental Science and Engineering, Shaanxi University of Science and Technology, Xi'an 710021 (P. R. China)

<sup>c</sup> Fourth Military Medical University, Xi'an 710032, China

<sup>d</sup> College of Life Sciences, Northwest University, Xi'an 710069, China

†Electronic Supplementary Information (ESI) available: See DOI: 10.1039/x0xx00000x

## Experimental Procedures

**Preparation of g-C<sub>3</sub>N<sub>4</sub>(CN):** Melamine was purchased from Sinopharm Chemical Reagent Co., Ltd. All chemicals were analytical grade and used without further purification. Briefly, 4 g of melamine was put into a covered quartz crucible, which was placed in a muffle furnace. Then, this quartz crucible was heated to 520 °C (The heating rate was 5 °C/min) and kept for 4 hours. When the temperature of the furnace is reduced to room temperature, it can be found that the melamine has changed to a yellow honeycombed mass. After the grinding, washing, and drying, this yellow honeycombed mass was changed to yellow powder. This powder is a g-C<sub>3</sub>N<sub>4</sub> sample (CN).

**Preparation of NaOH solution:** NaOH solid (NaOH) was purchased from Shanghai Titan Co., Ltd. It was analytical grade and used without further purification. Typically, 4 g of NaOH is dispersed into 100 mL of deionized water and stirred until all the NaOH particles were dissolved. Then, a 1 mol/L NaOH solution was obtained.

**Preparation of terephthalic (PTA) acid solution:** 0.4 g of NaOH and 1000 mL of deionized water were added to a beaker. Then, 0.83 g of PTA was also added to his beaker, which was heated (50 °C) in water bath equipment under magnetic stirring (400 r/min) for 24 h.

**NO removal experiments:** Before the NO removal experiments, the sample dish should be prepared. First, 50 mg of the catalyst was dispersed in 10 ml of deionized water and then dispersed evenly via supersonic dispersion for 15 min. The catalyst suspension was poured into a glass dish (R = 3 cm) and dried in an oven at 60 °C. The photothermal unit is then connected in the sequence shown in Figure S1, the sample tray is placed in the photothermal catalytic unit, the temperature is adjusted and air and NO are introduced, a xenon lamp is used as the visible light source, and the effluent gas is detected by a NO<sub>x</sub> analyzer and the final exhaust gas is collected by a wet absorption unit.

**Reaction constants, Ea, and NO<sub>2</sub> selectivity calculations:** The reaction constants were calculated according to equation 1, C is the real-time NO concentration and C<sub>0</sub> is the initial NO concentration; Ea was calculated according to equation 2 (Arrhenius formula), k is the rate constant, R is the molar gas constant, R = 8.314472J/ (mol·K), T is the thermodynamic temperature and A is the prefactor; NO<sub>2</sub> selectivity (μ) was calculated according to equation 3, C<sub>NO<sub>2</sub></sub> is the concentration detected by the NO<sub>x</sub> analyzer during the reaction and C<sub>NO</sub> is the NO consumption concentration.

- (1)  $\ln(C/C_0) = -kt$ ;
- (2)  $\ln k = Ea/RT + C$ ,  $A = e^C$ ;
- (3)  $\mu = C_{NO_2}/C_{NO}$ .

**Species capture experiment:** In the NO removal process, the electrons (e<sup>-</sup>), holes (h<sup>+</sup>), hydroxyl radicals (·OH), and superoxide radicals (·O<sub>2</sub><sup>-</sup>) were captured using potassium iodide (50 mg), potassium dichromate (50 mg), tert-butanol (1 mL) and p-benzoquinone (50 mg), respectively. Each of these capturing agents is mixed with CN (50mg) to make a sample dish. The experimental procedure for the capture of active species was the same as that for the photocatalytic activity measurements.<sup>[1]</sup>

**The apparent quantum yields (AQYs):** AQYs were calculated by the following equations, and the intensity of incident light was measured by a PL-MW200 photoradiometer (Perfect Light, Beijing, China). I is the light intensity, and the test value is 782.2 mW; A is the area of the light spot, and the test value is 86.5 cm<sup>2</sup>; h is the Planck constant; NA is the Avogadro constant; v is the photon frequency, and the wavelength is 420 nm.

$$(1) \text{ The consumption of NO (C}_{NO}\text{): } C_{NO} = \sum_{t=1}^{t=30} NOc = 7200 \text{ ppb} = 7.2 \text{ ppm.}$$

The concentration of consumption NO ( $C_{NO}$ ) is:  $C_{NO} = \frac{7.2}{22.4} = 0.32 \mu\text{mol/L}$ .

(2) At room temperature  $20^\circ\text{C}$ , the concentration NO which is converted to  $\text{HNO}_3$

( $C_{NO/\text{HNO}_3}$ ) is:

$$C_{\text{NO}_3^-} = \frac{4.83}{22.4} = 0.22 \mu\text{mol/L}.$$

(3) photon number is:  $N(\text{photo}) = \sum_{t=1}^{t=30} I \times \frac{A}{h \times \nu} = 2.58 \times 10^{19}$  photons/min.

(4) The corresponding conversion of a NO molecule into a  $\text{NO}_3^-$  transfers 3 electrons, so the factor in front of the  $\text{NO}_3^-$  concentration is 3. So the apparent quantum yields of CN are:

$$\Phi_{\text{T}20} = \frac{3 \times C(\text{NO}_3^-) \times NA}{N(\text{photo})} \times 100\% = 1.54\%.$$

(5) Under the  $150^\circ\text{C}$ , the apparent quantum yields of CN is:

$$\Phi_{\text{T}150} = \frac{3 \times C(\text{NO}_3^-) \times NA}{N(\text{photo})} \times 100\% = 1.84\%.$$

(6) Under the  $150^\circ\text{C}$ , the apparent quantum yields of CN is:

$$\Phi_{\text{T}300} = \frac{3 \times C(\text{NO}_3^-) \times NA}{N(\text{photo})} \times 100\% = 2.22\%.$$

**Ion Chromatography Testing:** The reacted sample was washed down with 10ml of deionized water, added to a 10ml test tube and sonicated for 10min, centrifuged, and filtered to obtain the supernatant, which was tested by ion chromatography to obtain the  $\text{NO}_3^-$  concentration in the reacted sample. Similarly, 10 ml of the solution in the post-reaction tail gas absorption unit was taken and tested using ion chromatography. The ion chromatography model is the ICS-5000.

**The detection of active species:** First, 50 mg of the CN samples were dispersed in 10 ml of deionized water and dispersed evenly in an ultrasonic bath for 15 min. Then, the sample suspension was poured into a glass dish and dried in an oven at  $60^\circ\text{C}$  to form a sample dish. This sample dish is then placed in the middle of the photothermal reactor, while air flows through the air tube to contact the sample inside the reactor. A xenon lamp is selected as the visible light source and the visible light is directed onto the  $\text{g-C}_3\text{N}_4$  surface through a circular quartz skylight. After half an hour of visible light

irradiation, the sample dish was taken out and washed with 4ml of terephthalic acid solution (1.25 mmol/L). Then, the supernatant was extracted via ultrasonic centrifugation. Finally, the  $\cdot\text{OH}$  concentration was measured by a fluorescence spectrophotometer (emitted at 426 nm and excited at 312 nm).

**The detection of free radicals:** A Bruker EMX PLUS instrument was used for the electron paramagnetic resonance (EPR) experiments. Samples for EPR measurement were carried out by using DMPO (5,5-dimethyl-1-pyrroline N-oxide) as the spin trapping agent, mixing the samples (10 mg) in a 40 mM DMPO solution tank (Methanol dispersion for  $\cdot\text{O}_2^-$ ). Then, the suspension was irradiated with visible light or 550nm green light for 5 min (the suspension was irradiated with visible light and heated at 353K for 5 min). In the detection process, the modulation frequency was 100 kHz; the modulation amplitude was 1 G; the sweep time was 30 s; the field position was 3502 G; the center field was 3502 G; the attenuation was 15 dB.

**Temperature programmed desorption test for  $\text{NO}_2$ -TPD:** The 50 mg sample was weighed and placed in a reaction tube. Then, the sample was heated to 300°C with a heating rate of 10°C/min. Subsequently, an  $\text{N}_2$  flow (30 mL/min) was introduced into the reaction tube to purge the sample until the temperature of the sample was cooled to 50°C. This process was used to remove the gases that were originally adsorbed on the surface of the sample. After this process, a stream of  $\text{N}_2$  with 10%  $\text{NO}_2$  flowed through (30 mL/min) the sample for 1 hour to achieve the saturation adsorption of  $\text{NO}_2$ . The unabsorbed  $\text{NO}_2$  was removed from the surface of the sample via the  $\text{N}_2$  (100%) purging (30 mL/min). Finally, the temperature of the sample was increased from room temperature to 400°C at a heating rate of 10°C/min in the  $\text{N}_2$  atmosphere, and the desorbed  $\text{NO}_2$  was detected by the thermal conductivity detector (TCD, AutoChem1 II 2920).

**Photoelectrochemical experiment:** To test the photovoltaic properties of the catalyst, the catalyst was made in the form of a thin film and the experimental sample was chosen to be CN. Firstly, 20 mg of CN sample and 400uL of absolute ethanol were taken into a 2 ml test tube sonicated for 15 minutes to make the powder evenly dispersed. Secondly, the FTO glasses were cut into the size of 2.5\*2.5 cm, and a non-conductive channel about 90  $\mu\text{m}$  wide by a glass cutter was cut in the middle of the FTO glasses. The scribed FTO was cleaned and the paste was applied to the surface of the FTO to dry into a film. Finally, it was placed in a muffle furnace for calcination at 500 °C for 1 h to obtain the final film.

The heating unit and electrochemical workstation were then connected as shown in Figure S2. The sample was placed in a closed stainless-steel reactor, the interior of the reactor was pumped into a vacuum with an air pump, 100 ml of  $\text{N}_2$  ( $\text{O}_2$ ) was injected

with a gas needle, the temperature was controlled with a heating jacket, a xenon lamp was used as the lamp source and the sample film was irradiated through a quartz skylight for photocurrent testing.<sup>[2]</sup>

**Density functional theory (DFT) calculations:** DFT calculations were performed using the Gaussian 09 package program.<sup>[3-5]</sup> The electrostatic potential diagram and frontier orbital distribution diagram of the molecular fragments were plotted by visual molecular dynamics (VMD) program.<sup>[6]</sup> The PBE0/611G (d, p) functional method was used to simulate the intermolecular adsorption. Multiwfn 3.7 program and GaussView6.0 package were also used for analysis and plotting. The adsorption energy (E<sub>ads</sub>) is defined as

$$E_{ads} = E_{tot} - (E_{CN} + E_{mol})$$

Where E<sub>tot</sub>, E<sub>CN</sub> and E<sub>mol</sub> are the total energy of the adsorption complex, the pure CN and the isolated molecules, respectively.

**Sample characterization:** To test the crystal structure of the samples after reaction at different temperatures, X-ray diffraction (XRD) measurements were performed with a Bruker D8 diffractometer at Angle 10-80 (2θ) with an acceleration voltage of 40 kV and a current of 40 mA. To test the crystal structure of samples at different temperatures, in-situ X-ray diffraction (XRD) tests were performed with a Neo-Confucianism Smartlab diffractometry at an Angle of 10-80 (2θ) with an acceleration voltage of 40 kV and a current of 40 mA. To test the stability of the sample at high temperature, the sample was tested with a heating rate of 10 °C/min, and the whole testing process was recorded. The thermogravimetric instrument used is TGA55. The light absorption capacity of the samples was analyzed by a UV-visible spectrophotometer (Shimadzu UV-2600) and tested in situ by UV Shimadzu 3600Plus. To investigate the separation efficiency of the photogenerated electron and hole pairs, fluorescence emission spectra (PL) of samples were measured with Edinburgh FLS980 (UK) under different temperatures. The excitation wavelength is 345 nm.

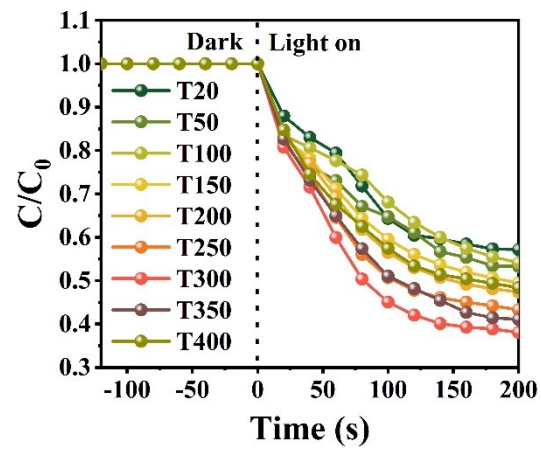
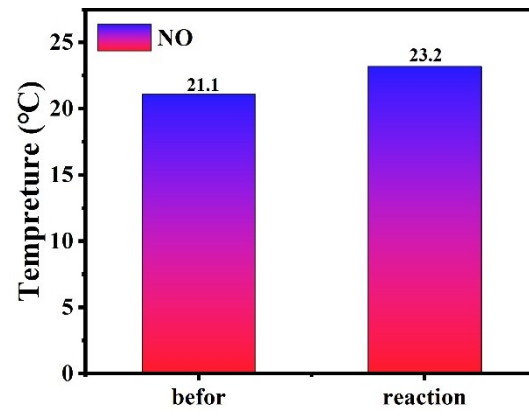


Fig. S1. NO removal efficiency of CN photothermal catalysis.



**Fig. S2.** Gas temperature before and after photothermal catalytic removal of NO reaction.

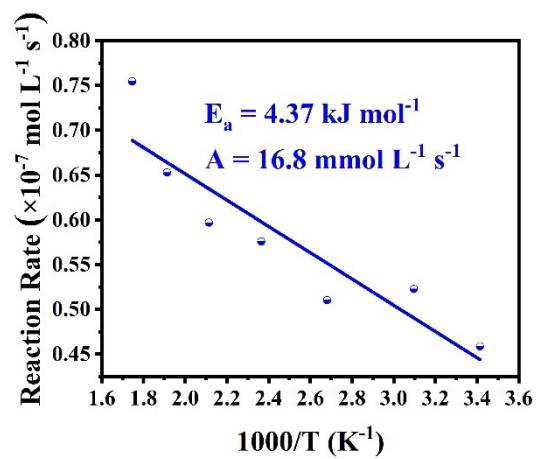


Fig. S3. Temperature and reaction rate relationship.



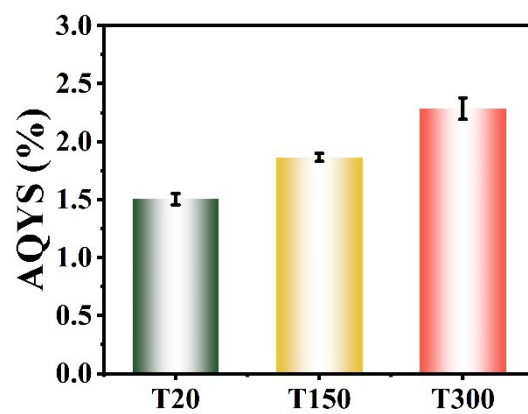


Fig. S4. Histogram of apparent quantum yields at different temperatures.

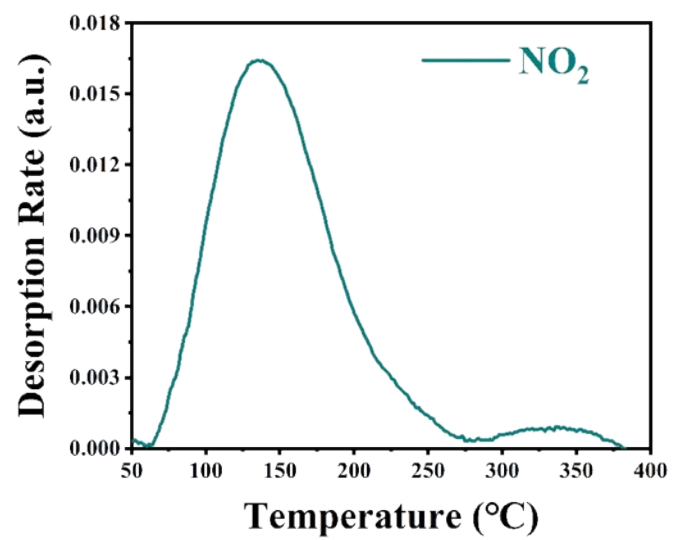


Fig. S5. NO<sub>2</sub> TPD of CN



Fig. S6. KNO<sub>3</sub> evaporation crystallization process.

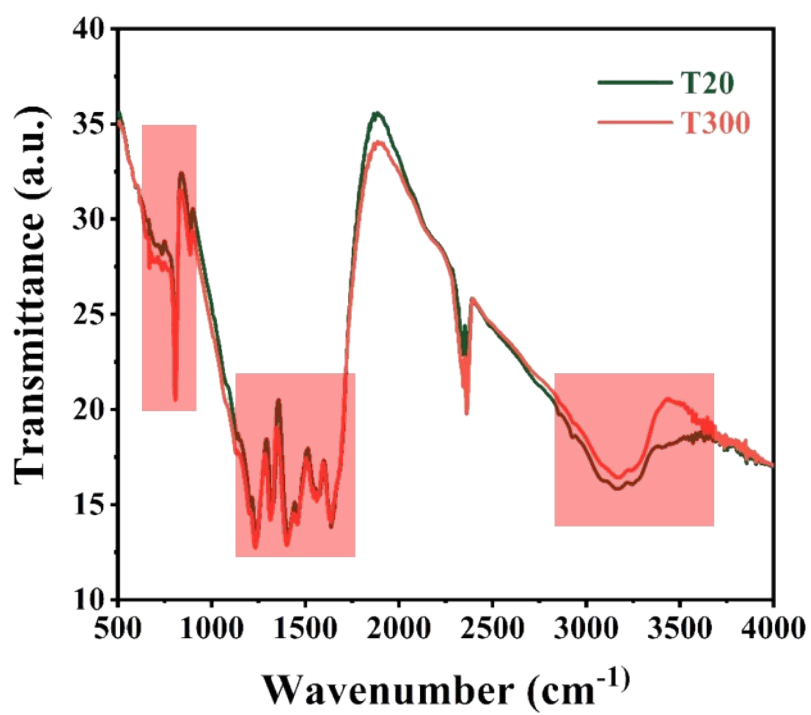


Fig. S7. In situ FT-IR of CN at different temperatures.

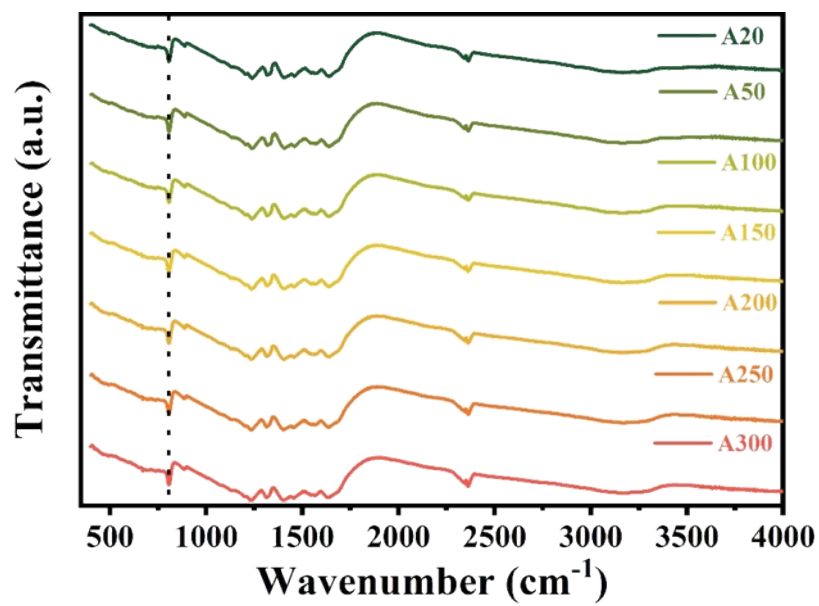


Fig. S8. FT-IR of CN at room temperature after reaction at different temperatures.

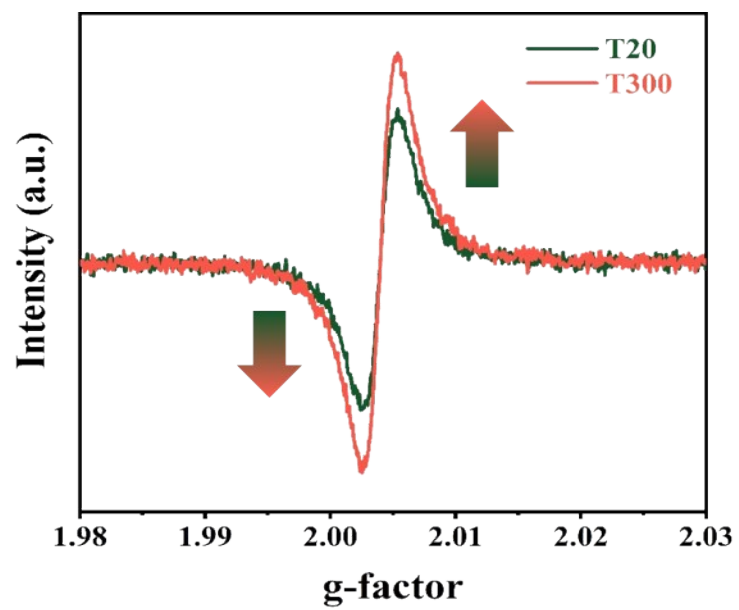


Fig. S9. In-suit EPR spectra of CN.

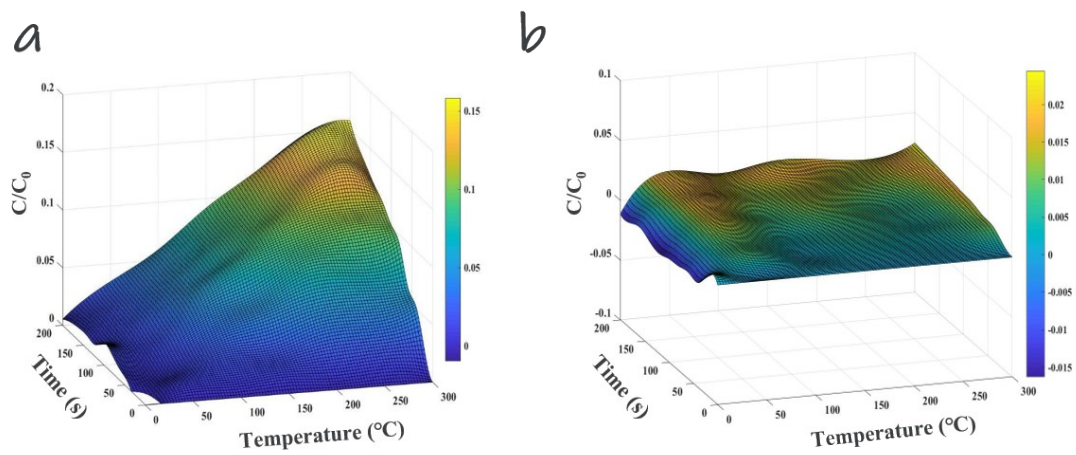


Fig. S10. Photothermal catalytic removal of NO under 550nm (a) and 650nm (b) light.

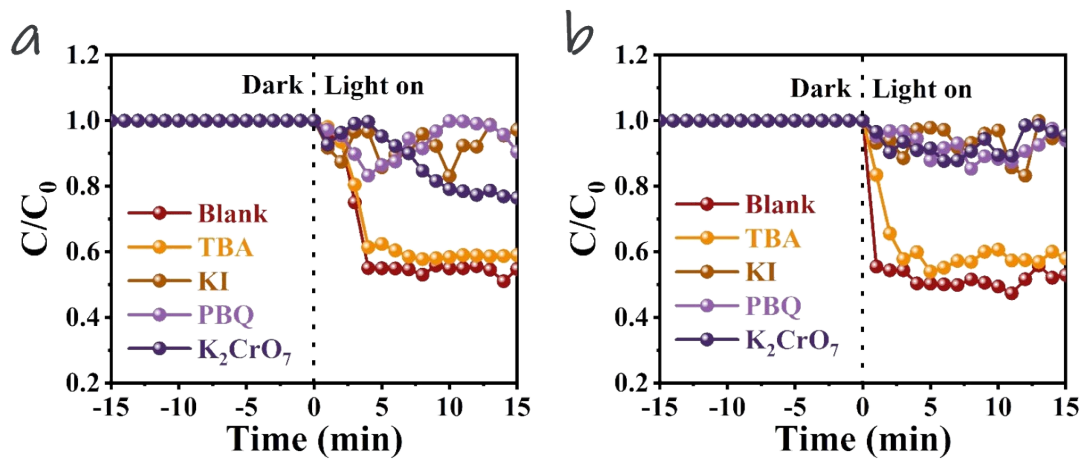


Fig. S11. Photocatalytic NO removal and capture experiments at room temperature(a) and 150°C(b).



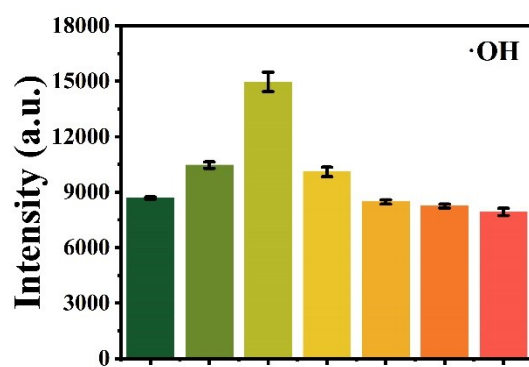


Fig. S12. Test the yield of  $\text{g-C}_3\text{N}_4 \cdot\text{OH}$  at different temperatures.

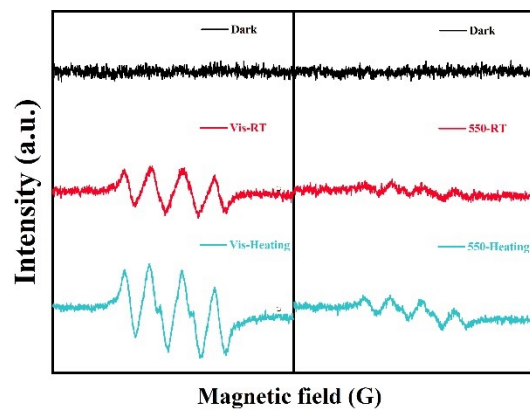
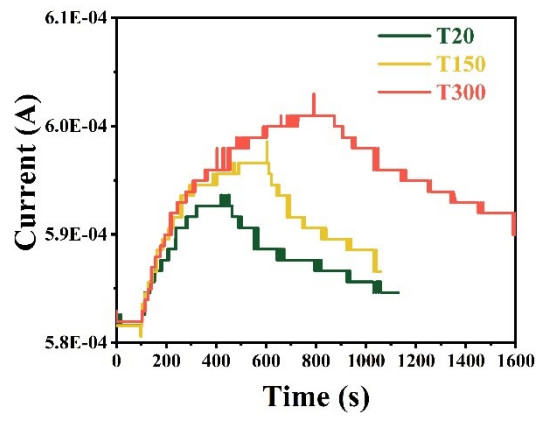


Fig. S13. ESR spectra of CN.



**Fig. S14.** In the Air atmosphere at different temperatures, real-time photocurrent curve.

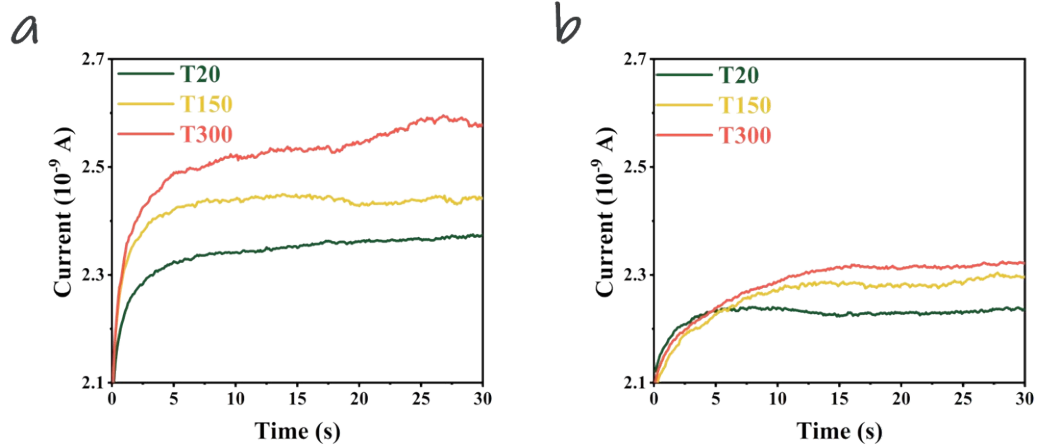


Fig. S15. In an  $N_2$  atmosphere (a) and  $O_2$  atmosphere (b) at different temperatures, the dark current of the sample is when the lamp is off.

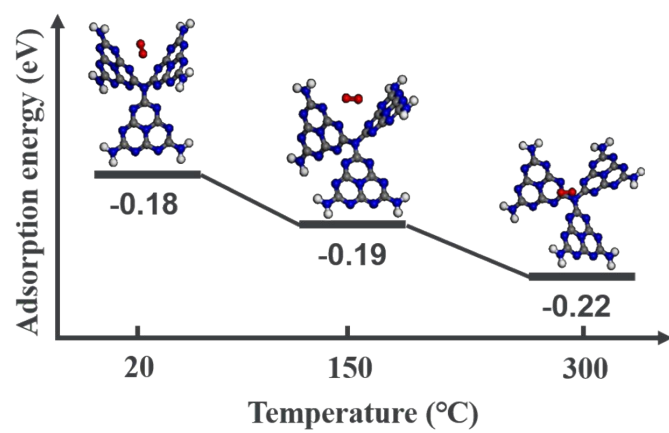


Fig. S16. The adsorption energy of O<sub>2</sub> on different CN structures.

Temperature(°C)	2 $\theta$ (Degree)	Interplanar Crystal Spacing(nm)
20	27.5411	0.08248
50	27.4104	0.08479
100	27.3620	0.08577
150	27.2313	0.08881
200	27.1442	0.09117
250	27.0522	0.09401
300	26.9651	0.09707

**Table S1.** Different temperatures correspond to the crystal plane spacing.

#### Reference

- [1] M. Zhou, G. Dong, F. Yu, and Y. Huang, *Appl. Catal. B Environ.*, 2019, **256**, 117825.
- [2] M. Wang, G. Tan, D. Zhang, B. Li, L. Lv, Y. Wang, and Y. Liu, *Appl. Catal. B Environ.*, 2019, **254**, 98-112.
- [3] M.J. Frisch, G.W. Trucks, H.B. Schlegel, G.E. Scuseria, M.A. Robb, J.R. Cheeseman, and H. Nakatsuji, Gaussian 09, revision D. 01, *Gaussian Inc.*, Wallingford, 2009, **121**, 150-166.
- [4] Z. Deng, J. Zhu, P. Li, Z. Du, X. Qi, X. Chen, R. Mu, C. Zeng, Y. Ma, and Z. Zhang, *J. Mol. Liq.*, 2023, **384**, 122283.
- [5] L. Sellaoui, D. I. Mendoza-Castillo, H. E. Reynel-Ávila, B. A. Ávila-Camacho, L. L. Díaz-Muñoz, H. Ghalla, A. Bonilla-Petriciolet, and A. B. Lamine, *Chem. Eng. J.*, 2019, **365**, 305.
- [6] W. Humphrey, A. Dalke, and K. Schulten, *J. Mol. Graph.*, 1996, **14**, 33.